International Journal of Modern Physics A

TeV Scale $B - L$ Phenomenology at LHC

M. Abbas[1,2], W. Emam[1], S. Khalil[1,2], and M. Shalaby[1]

[1] *Faculty of Science, Ain Shams University, Cairo 11566, Egypt.*
2 *Center for Theoretical Physics at the British University in Egypt, Cairo 11837, Egypt.*

We present the phenomenology of the low scale $U(1)_{B-L}$ extension of the standard model and its implications at LHC. We show that this model provides a natural explanation for the presence of three right-handed neutrinos and can naturally account the observed neutrino masses and mixing. We study the decay and production of the extra gauge boson and the SM singlet scalar (heavy Higgs) predicted in this type of models. We find that the cross sections of the SM-like Higgs production are reduced by $\sim 20\% - 30\%$, while its decay branching ratios remain intact. The extra Higgs has relatively small cross sections and the branching ratios of $Z' \to l^+ l^-$ are of order $\sim 20\%$ compared to $\sim 3\%$ of the SM results.

Keywords: Low scale $B-L$; Neutrino masses and mixing, Higgs production; Higgs decays; Z' gauge boson

1. Introduction

The search for New Physics at the TeV scale is a major goal of present and future colliders. The starting of the Large Hadron Collider (LHC) in 2008 brings closer the moment where the physics beyond the Standard Model (SM) can be explored.

The evidence for non-vanishing neutrino masses, based on the apparent observation of neutrino oscillation, suggests the extension of the gauge symmetry of the SM via $U(1)$ gauge symmetries beyond the hypercharge gauge symmetry, $U(1)_Y$. Several attempts have been already proposed to extend the SM gauge symmetry of the SM via one or more $U(1)$ [1,2,3].

In this type of models [1,2], three SM singlet fermions arise quite naturally due to the anomaly cancellation conditions. These three particles are accounted for right handed neutrinos, and hence a natural explanation for the seesaw mechanism is obtained.

Recent consideration of a low-scale $B - L$ symmetry-breaking model, based on the gauge group $G_{B-L} \equiv SU(3)_C \times SU(2)_L \times U(1)_Y \times U(1)_{B-L}$, predicts an extra SM singlet scalar (extra Higgs) and one extra neutral gauge boson corresponding to $B - L$ gauge symmetry [2]. Because these new particles may have significant impact on the SM phenomenology, they may lead to interesting signatures at the LHC.

The paper is aimed at studying the Higgs boson production and decay rates at the LHC in this minimal U(1)(B-L) extension of the Standard Model with an extra

SM singlet Higgs boson. The study is carried out in a maximal-mixing scenario for the two physical Higgs bosons, H and H, and for the minimal experimentally allowed mass (i.e., 600 GeV) of the extra Z gauge boson.

We show that the cross sections of the Higgs production are reduced by $\sim 20\% - 30\%$ in the interesting mass range of $\sim 120 - 250$ GeV relative to the SM predictions. However, its decay branching ratios remain intact. In addition, we find that the extra Higgs ($\sim$ TeV) is accessible at LHC, although it has relatively small cross sections. We also examine the availability of the decay channel $H' \to HH$, which happens to have very small partial decay width. Concerning the Z' gauge boson, the branching ratios of $Z' \to l^+l^-$ are found to be of order $\sim 20\%$ compared to $\sim 3\%$ of the SM $BR(Z \to l^+l^-)$.

This paper is organized as follows. In section 2 we review the Higgs mechanism and symmetry breaking within the minimal $B - L$ extension of the SM. We also discuss the mixing between the SM-like Higgs and the extra Higgs boson. In Section 4 we present the phenomenology of the two Higgs particles. The production cross sections and decay branching ratios of these Higgs particles at LHC are analyzed. In section 5 we study the decay of the extra gauge boson Z'. Section 6 contains the Conclusions.

2. $B - L$ extension of the SM

2.1. *Symmetry breaking*

The $B-L$ model under consideration can be described by the following Lagrangian

$$\begin{aligned}\mathcal{L}_{B-L} = & \, i\,\bar{l}D_\mu\gamma^\mu l + i\,\bar{e}_R D_\mu\gamma^\mu e_R + i\,\bar{\nu}_R D_\mu\gamma^\mu\nu_R \\ & -\frac{1}{4}W_{\mu\nu}W^{\mu\nu} - \frac{1}{4}B_{\mu\nu}B^{\mu\nu} - \frac{1}{4}C_{\mu\nu}C^{\mu\nu} \\ & +(D^\mu\phi)(D_\mu\phi) + (D^\mu\chi)(D_\mu\chi) - V(\phi,\chi) \\ & -\Big(\lambda_e\bar{l}\phi e_R + \lambda_\nu\bar{l}\tilde{\phi}\nu_R + \frac{1}{2}\lambda_{\nu_R}\bar{\nu^c}_R\chi\nu_R + h.c.\Big),\end{aligned} \tag{1}$$

where the covariant derivative D_μ is different from the SM one by the term $ig''Y_{B-L}C_\mu$. Here g'' is the $U(1)_{B-L}$ gauge coupling constant, Y_{B-L} is the $B-L$ charge, and $C_{\mu\nu} = \partial_\mu C_\nu - \partial_\nu C_\mu$ is the field strength of the $U(1)_{B-L}$. The Y_{B-L} for fermions and Higgs are given in Table 1. λ_e, λ_ν and λ_{ν_R} refer to 3×3 Yakawa matrices. The interaction terms $\lambda_\nu l\tilde{\phi}\nu_R$ and $\lambda_{\nu_R}\bar{\nu^c}_R\chi\nu_R$ give rise to a Dirac neutrino mass term: $m_D \simeq \lambda_\nu v$ and a Majorana mass term: $M_R = \lambda_{\nu_R}v'$, respectively. $U(1)_{B-L}$ and $SU(2)_L \times U(1)_Y$ gauge symmetries are spontaneously broken by a SM singlet complex scaler field χ and a complex $SU(2)$ doublet of scalar fields ϕ, respectively.

The most general Higgs potential invariant under these symmetries is given by

$$\begin{aligned}V(\phi,\chi) = & \, m_1^2\phi^\dagger\phi + m_2^2\chi^\dagger\chi + \lambda_1(\phi^\dagger\phi)^2 + \lambda_2(\chi^\dagger\chi)^2 \\ & +\lambda_3(\chi^\dagger\chi)(\phi^\dagger\phi),\end{aligned} \tag{2}$$

Table 1. $B-L$ quantum numbers for fermions and Higgs particles.

particle	l	e_R	ν_R	q	ϕ	χ
Y_{B-L}	-1	-1	-1	$1/3$	0	2

where $\lambda_3 > -2\sqrt{\lambda_1\lambda_2}$ and $\lambda_1, \lambda_2 \geq 0$, so that the potential is bounded from below. For non-vanishing vacuum expectation values (vev's), we require $\lambda_3^2 < 4\lambda_1\lambda_2$, $m_1^2 < 0$ and $m_2^2 < 0$. The vev's, $|\langle\phi\rangle| = v/\sqrt{2}$ and $|\langle\chi\rangle| = v'/\sqrt{2}$, are then given by

$$v^2 = \frac{4\lambda_2 m_1^2 - 2\lambda_3 m_2^2}{\lambda_3^2 - 4\lambda_1\lambda_2}, \qquad v'^2 = \frac{-2(m_1^2 + \lambda_1 v^2)}{\lambda_3}.$$

Depending on the value of the λ_3 coupling, one can have $v' \gg v$ or $v' \approx v$. Therefore, the symmetry breaking scales, v and v', can be responsible for two different symmetry breaking scenarios. In our analysis we take $v = 246$ GeV and constrain the other scale, v', by the lower bounds imposed on the mass of the extra neutral gauge boson.

The gauge field C_μ (will be called Z' in the rest of the paper) acquires its mass once the the $B-L$ gauge symmetry is broken:

$$m_{Z'}^2 = 4g''v'^2. \tag{3}$$

The experimental search for Z' at LEP II gives the strongest limit[6]

$$m_{Z'}/g'' > 6TeV. \tag{4}$$

Thus if the coupling g'' is $< O(1)$, one can get $m_{Z'} \gtrsim O(600)$ GeV.

2.2. *Higgs sector*

The SM complex $SU(2)_L$ doublet and the extra complex scalar singlet arise in this class of models, give six scalar degrees of freedom. Only two physical degrees of freedom, (ϕ, χ), remain after the $B-L$ and electroweak symmetries are broken. The other four degrees of freedom are eaten by Z', Z and $W^\pm$ bosons.

As previously stated, two different symmetry breaking scenarios can be obtained in this class of models. For positive λ_3, one finds that $v' >> v$. In this case, the SM singlet Higgs, ϕ, and the SM like Higgs, χ, are decoupled and their masses are given by

$$M_\phi = \sqrt{2\lambda_1}v, \qquad M_\chi = \sqrt{2\lambda_2}v'. \tag{5}$$

For negative λ_3, however, $v' \sim v$. In this scenario, a significant mixing between the two Higgs scalars exists and can affect the SM phenomenology. This mixing can be represented by the following mass matrix for ϕ and χ:

$$\frac{1}{2}M^2(\phi,\chi) = \begin{pmatrix} \lambda_1 v^2 & \frac{\lambda_3}{2}vv' \\ \frac{\lambda_3}{2}vv' & \lambda_2 v'^2 \end{pmatrix}. \tag{6}$$

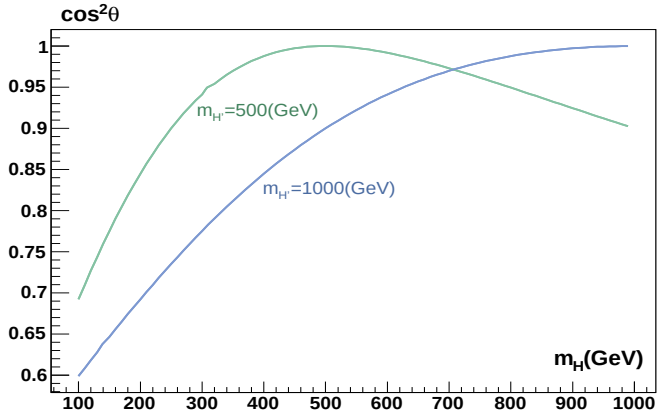

Fig. 1. $H - H'$ mixing angle as function of m_H for $m'_H = 500$ GeV and 1 TeV.

Therefore, the mass eigenstates fields H and H' are given by the following equation:

$$\begin{pmatrix} H \\ H' \end{pmatrix} = \begin{pmatrix} \cos\theta & -\sin\theta \\ \sin\theta & \cos\theta \end{pmatrix} \begin{pmatrix} \phi \\ \chi \end{pmatrix}, \tag{7}$$

where the mixing angle θ is defined by

$$\tan 2\theta = \frac{|\lambda_3| v v'}{\lambda_1 v^2 - \lambda_2 v'^2}. \tag{8}$$

The masses of H and H' are therefore given by the following formula:

$$m^2_{H,H'} = \lambda_1 v^2 + \lambda_2 v'^2 \mp \sqrt{(\lambda_1 v^2 - \lambda_2 v'^2)^2 + \lambda_3^2 v^2 v'^2}. \tag{9}$$

H and H' are called light and heavy Higgs bosons, respectively.

To reduce the number of free parameters in this model, a maximum mixing between the two Higgs bosons is considered by taking $|\lambda_3| \simeq \lambda_1^{\max} \lambda_2^{\max}$, where $\lambda_1^{\max}$ and $\lambda_2^{\max}$ are given by

$$\begin{aligned} \lambda_1^{\max} &= \frac{m_H^2 + m_{H'}^2 - \sqrt{4 m_H^2 m_{H'}^2 + 1} + 1}{4v^2}, \\ \lambda_2^{\max} &= \frac{m_H^2 + m_{H'}^2 + \sqrt{4 m_H^2 m_{H'}^2 + 1} - 1}{4v'^2}, \end{aligned} \tag{10}$$

and the maximum mixing angle is then given by

$$\tan 2\theta = \frac{\lambda_1^{\max} \lambda_2^{\max} v v'}{\lambda_1^{\max} v^2 - \lambda_2^{\max} v'^2}. \tag{11}$$

If the vev's are fixed at $v = 246$ GeV and $v' = 1$ TeV and one takes $m_{Z'} \gtrsim O(600)$ GeV, the number of free parameters in this model are further reduced into only two m_H and $m_{H'}$. In Figure 1, we present the maximum mixing as a function of the light Higgs mass, m_H for $m_{H'} = 500$ GeV and 1 TeV.

The mixing between the two Higgs bosons of this model modifies the usual couplings among the SM-like Higgs, H, and the SM fermions and gauge bosons. Moreover, new couplings are produced among the extra Higgs, H', and the SM particles:

$$\begin{aligned} g_{Hff} &= i\frac{m_f}{v}\cos\theta, \quad g_{H'ff} = i\frac{m_f}{v}\sin\theta, \\ g_{HVV} &= -2i\frac{m_V^2}{v}\cos\theta, \quad g_{H'VV} = -2i\frac{m_V^2}{v}\sin\theta, \\ g_{HZ'Z'} &= 2i\frac{m_C^2}{v'}\sin\theta, \quad g_{H'Z'Z'} = -2i\frac{m_C^2}{v'}\cos\theta, \\ g_{H\nu_R\nu_R} &= -i\frac{m_{\nu_R}}{v'}\sin\theta, \quad g_{H'\nu_R\nu_R} = i\frac{m_{\nu_R}}{v'}\cos\theta. \end{aligned} \tag{12}$$

The Higgs self couplings are give by

$$\begin{aligned} g_{H^3} &= 6i(\lambda_1 v\cos^3\theta - \frac{\lambda_3}{2}v'\cos^2\theta\sin\theta), \\ g_{H'^3} &= 6i(\lambda_2 v'\cos^3\theta + \frac{\lambda_3}{2}v\cos^2\theta\sin\theta), \\ g_{H^4} &= 6i\lambda_1\cos^4\theta, \\ g_{H'^4} &= 6i\lambda_2\cos^4\theta, \\ g_{HH'^2} &= 2i(\frac{\lambda_3}{2}v\cos^3\theta + \lambda_3 v'\cos^2\theta\sin\theta - 3\lambda_2 v'\cos^2\theta\sin\theta), \\ g_{H^2H'} &= 2i(\frac{\lambda_3}{2}v'\cos^3\theta - \lambda_3 v\cos^2\theta\sin\theta + 3\lambda_1 v\cos^2\theta\sin\theta), \\ g_{H^2H'^2} &= i\lambda_3\cos^4\theta. \end{aligned} \tag{13}$$

These new couplings lead to a different Higgs phenomenology from the well known one, predicted by the SM. The detailed analysis of Higgs bosons in this class of models and their phenomenological implications, like their productions and decays at the LHC, will be discussed in the next section.

The detailed analysis of Higgs bosons production and decay in model and their phenomenological implications at the LHC will be discussed in the next two sections.

3. Neutrino Masses and Mixing

In this section we provide a detail analysis for the neutrino masses and mixing in the gauge $B-L$ extension of the SM, where the neutrino masses may be generated through a TeV scale seesaw mechanism [7]. After $U(1)_{B-L}$ symmetry breaking, the Yukawa interaction term: $\frac{1}{2}\lambda_{\nu_R}\bar{\nu_R^c}\chi\nu_R$ gives rise to the right handed neutrino mass:$M_R = \frac{1}{2\sqrt{2}}\lambda_{\nu_R}v'$. On the other hand, the Dirac neutrino mass $m_D = \frac{1}{\sqrt{2}}\lambda_\nu v$ arises from the Yukawa term $\lambda_\nu\bar{l}\tilde{\phi}\nu_R$ due to the electroweak symmetry breaking. Therefore, the mass matrix of the left and right-handed neutrino is given by

$$\begin{pmatrix} 0 & m_D \\ m_D & M_R \end{pmatrix}, \tag{14}$$

where $M_R > m_D$. The digitalization of the mass matrix leads to the following masses for the light and heavy neutrinos, respectively

$$m_{\nu_L} \simeq -m_D M_R^{-1} m_D^T, \tag{15}$$

$$m_{\nu_H} \simeq M_R. \tag{16}$$

This mechanism is known as the seesaw mechanism. Thus, $B-L$ gauge symmetry explains the presence of three right handed neutrinos and provide a natural framework for the seesaw mechanism. However, the scale of B-L and the mass M_R remain arbitrary.

In the usual seesaw mechanism, to get m_{ν_L} of order $10^{-2}eV$ the mass of the heavy neutrino must be of order $\sim 10^{14}Gev$. It is important to note that such a large scale may be necessary if the Dirac neutrino masses are assumed to be of order $\mathcal{O}(100)$ GeV. However, there is no any low energy evidence that indicates that the Dirac masses should be of that order. On the contrary, if one tries to establish a flavor symmetry between charged and neutral leptons as in quark sector between up and down, one finds that the Dirac neutrino masses must be very small, of order $\mathcal{O}(10^{-4})$ GeV. This implies that M_R of order TeV is quite acceptable, which is known as low scale seesaw mechanism.

In our analysis, we adopt the basis where the charged lepton mass matrix and the Majorana mass matrix M_R are both diagonal. Therefore, one can parameterize M_R as follows

$$M_R = M_{R_3} \begin{pmatrix} r_1 & 0 & 0 \\ 0 & r_2 & 0 \\ 0 & 0 & 1 \end{pmatrix}, \tag{17}$$

where

$$M_{R_3} = |\lambda_{\nu_{R_3}}| \frac{v'}{2\sqrt{2}} \tag{18}$$

and

$$r_{1,2} = \frac{M_{R_{1,2}}}{M_{R_3}} = \left| \frac{\lambda_{\nu_{R_{1,2}}}}{\lambda_{\nu_{R_3}}} \right|. \tag{19}$$

As can be seen from Eq.(17) that even if v' is fixed to be of order TeV, the absolute value of M_R is still parameterized by three unknown parameters. On the other hand, the Dirac mass matrix (if it is real) is given in terms of 9 parameters. Since $U(1)_{B-L}$ can not impose any further constraint to reduce the number of these parameters, the total number of free parameters involved in the light neutrino mass matrix are 12 parameters. However, the solar and atmospheric neutrino oscillation experiments provide measurements of the neutrino mass-squared differences and the neutrino

mixing angles. At the 3σ level, the allowed ranges are [8] :

$$\begin{aligned} \Delta m^2_{12} &= (7.9 \pm 0.4) \times 10^{-5}\text{eV}^2, \\ |\Delta m^2_{32}| &= (2.4 + 0.3) \times 10^{-3}\text{eV}^2, \\ \theta_{12} &= 33.9^\circ \pm 1.6^\circ, \\ \theta_{23} &= 45^\circ, \\ \sin^2\theta_{13} &\leq 0.048. \end{aligned} \tag{20}$$

Therefore, the number of the experimental inputs are at most six: three neutrino masses (assuming possible ansatze like hierarchy or degenerate) and three mixing angles (if we assume $\theta_{13} = 0$).

One of the interesting parametrization for the Dirac neutrino mass matrix is given by

$$m_D = U_{PMNS}\sqrt{m_\nu^{diag}}R\sqrt{M_R}, \tag{21}$$

where m_ν^{diag} is the physical neutrino mass matrix and U_{PMNS} is the lepton mixing matrix, and can be written as

$$U_{PMNS} = U_{23}(\theta_{23})U_{13}(\theta_{13},\delta)U_{12}(\theta_{12})I_\phi, \tag{22}$$

where the U_{ij} are matrices of rotations in the ij plane by angle θ_{ij} and δ is the Dirac CP-violating phase attached to 1-3 rotation. $I_\phi \equiv diag(1, e^{i\phi_1}, e^{i\phi_2})$ is the diagonal matrix of the Majorana CP-violating phases.

One has several choices to write the mixing matrix U_{PMNS} depending on the values of the angles θ_{ij}. An interesting example the tri-bimaximal mixing

$$U_{PMNS} = U_{tbm}, \tag{23}$$

where the mixing angles are given by

$$\sin^2\theta_{12} = 1/3, \qquad \theta_{23} = \frac{\pi}{4}, \qquad \theta_{13} = 0, \tag{24}$$

or explicitly,

$$U_{tbm} = \frac{1}{\sqrt{6}}\begin{pmatrix} 2 & \sqrt{2} & 0 \\ -1 & \sqrt{2} & \sqrt{3} \\ 1 & -\sqrt{2} & \sqrt{3} \end{pmatrix}. \tag{25}$$

The matrix R is an arbitrary orthogonal matrix which can be in general parameterized in terms of three complex angles. Let us consider the following parametrization for R

$$R = \begin{pmatrix} c_2c_1 & s_1c_2 & s_2 \\ -s_1c_3 - c_1s_2s_3 & c_1c_3 - s_1s_2s_3 & s_1c_2 \\ s_1s_3 - c_3s_2c_1 & -c_1s_3 - s_1s_2c_3 & c_3c_2 \end{pmatrix} \tag{26}$$

where $c_i = cos(\theta_i + i\delta_i)$ and $s_i = sin(\theta_i + i\delta_i)$, $i = 1, 2, 3$ with δ_i are the phases associate with the matrix R. These phases are very relevant for non vanishing leptogenesis asymmetry.

In Eq.(21), the six unknown parameters are now given in terms of three masses in M_R and the three angles in R. In order to fix these angles, one needs a flavor symmetry beyond the gauge symmetry, which is typically flavor blind. Several types of flavor symmetries have been discussed in the literatures [9]. Here we follow different approach. We attempt to extend the observed relations between the masses of up quarks and charged leptons to the down quark and neutrino masses.

From the measured values of the up quark and charged lepton masses at the electroweak scale, one can notice the following relations

$$\frac{m_u}{m_c} \sim \frac{m_e}{m_\mu} \sim O(10^{-3}), \tag{27}$$

and

$$\frac{m_c}{m_t} \sim \frac{{m_\mu}^2}{{m_\tau}^2} \sim O(10^{-3}). \tag{28}$$

In the event of a flavor symmetry that explains these ratios, the down quark and neutrino sectors may also be subjected to this symmetry. Hence, a similar relation may be obtained among their masses. If the scale of this flavor symmetry breaking (v_F) is below seesaw ($B - L$ symmetry breaking) scale, then the above mass ratio would be extended to the down quark and light neutrino masses. In this case, one would expect that

$$\frac{m_d}{m_s} \sim \frac{m_{\nu_1}}{m_{\nu_2}} \sim O(10^{-2}) \tag{29}$$

$$\frac{m_s}{m_b} \sim \frac{m_{\nu_2}^2}{m_{\nu_3}^2} \sim O(10^{-2}). \tag{30}$$

However, if the scale of the flavor symmetry breaking is above the seesaw mechanism scale, then the mass ration is anticipated to be between down quark and Dirac neutrino masses, *i.e.*,

$$\frac{m_d}{m_s} \sim \frac{m_{D_1}}{m_{D_2}} \sim O(10^{-2}) \tag{31}$$

$$\frac{m_s}{m_b} \sim \frac{m_{D_2}^2}{m_{D_3}^2} \sim O(10^{-2}) \tag{32}$$

Let us start by considering the first scenario where $v_F < v'$. The experimental results for the light neutrino masses in Eq.(20) leads to

$$m_{\nu_2} = \sqrt{7.9 \times 10^{-5} - m_{\nu_1}^2}, \tag{33}$$

$$m_{\nu_3} = \sqrt{|2.4 \times 10^{-3} - 7.9 \times 10^{-5} + m_{\nu_1}^2|}, \tag{34}$$

with arbitrary m_{ν_1}. Thus, for $m_{\nu_1}^2 \ll 7.9 \times 10^{-5}$, the ansatz of hierarchal light neutrino masses is obtained. It is interesting to note that if $m_{\nu_1} \sim 10^{-4}$, the hierarchal ansatz is consistent with the mass relations given in Eqs.(29,30) and the light neutrino mass matrix takes the form

$$m_\nu \simeq 0.05\ eV \begin{pmatrix} 10^{-3} & 0 & 0 \\ 0 & 0.16 & 0 \\ 0 & 0 & 1 \end{pmatrix}. \tag{35}$$

The Dirac neutrino mass matrix is now given by (for $r_1 \sim r_2 \sim 0.1$, $M_{R_3} = 5$ TeV, and order one angles/phases of R-matrix):

$$m_D \simeq 10^{-3} \begin{pmatrix} 0.16 + 0.23\ i & -0.25 + 0.16\ i & -0.19 - 0.26\ i \\ -0.22 - 0.34\ i & 0.37 - 0.24\ i & 0.30 + 0.38\ i \\ -0.14 + 0.47\ i & -0.53 - 0.15\ i & 0.16 - 0.68\ i \end{pmatrix}. \tag{36}$$

Note that the complex phases in m_D are induced by the phases of R matrix since the mixing matrix U_{PMNS} is real ($\theta_{13} = 0$ is assumed). Also, as can be seen from the above example, $m_D \lesssim \mathcal{O}(10^{-4})$ GeV, hence the Yukawa coupling λ_ν is of order 10^{-6}, which is just one order of magnitude smaller than the electron Yukawa coupling.

Now we turn to the scenario of degenerate light neutrino masses ($m_{\nu_1} \simeq m_{\nu_2} \simeq m_{\nu_3} \simeq \tilde{m}$). From the astrophysical constraint: $\sum_i m_{\nu_i} < 1$ eV, one finds that $\tilde{m} < 0.3$ eV. Therefore,

$$m_{\nu_2} = \sqrt{\tilde{m}^2 + 7.9 \times 10^{-5}}, \tag{37}$$

$$m_{\nu_3} = \sqrt{\tilde{m}^2 + 2.4 \times 10^{-3} + 7.9 \times 10^{-5}}. \tag{38}$$

Thus, the light neutrino mass matrix takes the form

$$\begin{aligned} m_\nu &= \tilde{m} \begin{pmatrix} 1 & & \\ & \sqrt{1 + \frac{0.000079}{\tilde{m}^2}} & \\ & & \sqrt{1 + \frac{0.002479}{\tilde{m}^2}} \end{pmatrix} \\ &\lesssim 0.3\ \text{eV} \begin{pmatrix} 1 & & \\ & 1.00044 & \\ & & 1.01368 \end{pmatrix}. \end{aligned} \tag{39}$$

For $r_1 \sim r_2 \sim 1$ and $M_{R_3} = 10$ TeV, one finds the following neutrino Dirac mass matrix

$$m_D \simeq 10^{-2} \begin{pmatrix} -0.24 - 0.18\ i & 0.22 - 0.20\ i & -0.02 + 0.20\ i \\ -0.67 + 0.91\ i & -0.67 - 0.68\ i & 0.67 + 0.23\ i \\ 2.77 + 2.03\ i & -2.04 + 2.03\ i & 0.73 - 2.03\ i \end{pmatrix}. \tag{40}$$

Now we turn to the case of $v_F > v'$. From Eqs. (31,32), one gets

$$m_D^{diag} \simeq m_{D_3} \begin{pmatrix} 10^{-3} & 0 & 0 \\ 0 & 10^{-1} & 0 \\ 0 & 0 & 1 \end{pmatrix}. \tag{41}$$

If we assume hierarchal neutrino masses $m_{\nu_1} \ll m_{\nu_2} \ll m_{\nu_3}$, the light neutrino mass matrix can be written as

$$m_\nu \simeq 0.05\ eV \begin{pmatrix} m_{\nu_1} & 0 & 0 \\ 0 & 0.16 & 0 \\ 0 & 0 & 1 \end{pmatrix} \tag{42}$$

By using the determinant of m_D from Eqs.(21) and (41), one can express m_{D_3} in terms of m_{ν_1}, r_1, r_2 and M_{R_3} as follows:

$$\left(\frac{m_{D_3}}{\text{GeV}}\right) \simeq 10^{-4} \left(\frac{M_{R_3}}{\text{GeV}}\right)^{1/2} \left[r_1\ r_2 \left(\frac{m_{\nu_1}}{\text{eV}}\right)\right]^{1/6}. \tag{43}$$

Here, we have used the fact that the determinant of the orthogonal matrix R is one. Using this relation, one can determine, in terms of M_{R_3}, r_1 and r_2, the three angles $(\theta_1, \theta_2, \theta_3)$ and phases $(\delta_1, \delta_2, \delta_3)$ that parameterize the matrix R and lead to eigenvalues for the Dirac mass matrix m_D consistent with our inputs in Eq.(41).

In case of $r_1 \lesssim r_2 \lesssim 1$ (hierarchy heavy neutrino masses), one finds that there is a possible solution for the angles θ_i only for $m_{\nu_1} < 10^{-7}$ GeV. In addition the angle θ_3 can be fixed at $\theta_3 \simeq \pi/2$, hence the matrix R is given by

$$R = \begin{pmatrix} 0 & 0 & 1 \\ -\sin\alpha & \cos\alpha & 0 \\ -\cos\alpha & -\sin\alpha & 0 \end{pmatrix}, \tag{44}$$

where $\alpha = \theta_1 + \theta_2$. We find that the angle α is sensitive to r_2. In Figure 2, we plot the angle α as function of r_2 for $m_{R_3} = 5TeV$ and $r_1 \lesssim r_2$. Thus, the following R matrix is obtained

$$R = \begin{pmatrix} 0 & 0 & 1 \\ -0.6 & 0.8 & 0 \\ -0.8 & -0.6 & 0 \end{pmatrix}. \tag{45}$$

In case of degenerate heavy neutrino masses, *i.e.* $r_1 \simeq r_2 \simeq 1$, the matrix R is given by

$$R = \begin{pmatrix} 0 & 0 & 1 \\ -0.73 & 0.67 & 0 \\ -0.67 & -0.73 & 0 \end{pmatrix}. \tag{46}$$

Finally, we can also have a complex R, which induce a new source of CP violation phase in the Dirac Yukawa matrix Y_D. In this case, the angle α would be written as $\alpha = \rho + i\sigma$. For the above example of $r_1 = 0.1$ and $r_2 = 0.4$, the corresponding complex R-matrix is given by

$$R = \begin{pmatrix} 0 & 0 & 1 \\ -0.6\ e^{ia} & 0.8\ e^{ia} & 0 \\ -0.8\ e^{ia} & -0.6\ e^{ia} & 0 \end{pmatrix}. \tag{47}$$

It is important to mention that the complex phases in R matrix are not related to any of the low energy phases, however, it plays a crucial role in leptogenesis .

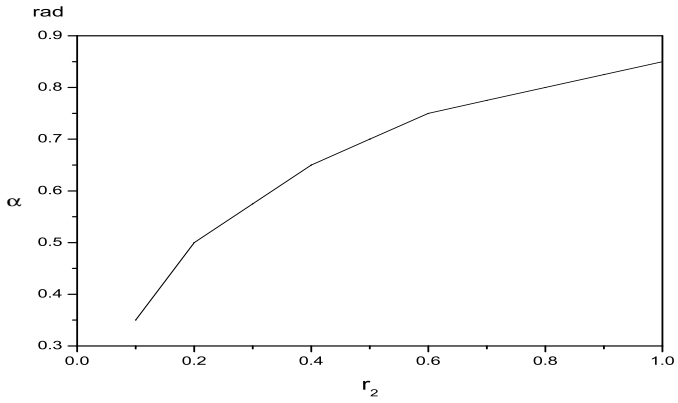

Fig. 2. The angle α verses $r_2 = \frac{M_{R_2}}{M_{R_3}}$ with $M_{R_3} = 5TeV$.

Before closing this section, we comment on the scenario of degenerate light neutrino masses ($m_{\nu_1} \simeq m_{\nu_2} \simeq m_{\nu_3} \simeq \tilde{m}$) in the case of $v_F > v'$. Here, the suggested mass relations between down type quark and neutrino masses should be implemented on the Dirac neutrino masses. However, we find that there is no any solution for the angles θ_{ij} that can account for the expected hierarchy of the Dirac neutrino eigenvalues. Therefore, in our framework, the ansatz of degenerate neutrino masses is disfavored .

4. Higgs Production and Decay at Hadron Colliders

4.1. *Higgs Production*

It is well known that at hadron colliders, the Higgs boson couples mainly to the heavy particles: the massive gauge bosons Z', Z and $W^{\pm}$ and the heavy quarks t, b. The main production mechanisms for Higgs particles can be classified into four groups [10]: the gluon–gluon fusion mechanism[11], the associated Higgs production with heavy top or bottom quarks[12], the associated production with $W/Z/Z'$ bosons[13], and the weak vector boson fusion processes[14]:

$$gg \to H \tag{48}$$

$$gg, q\bar{q} \to Q\bar{Q} + H, \tag{49}$$

$$q\bar{q} \to V + H \tag{50}$$

$$qq \to V^*V^* \to qq + H. \tag{51}$$

The Feynman diagrams corresponding to these processes are displayed in Figure 3. In case of the gluon–gluon fusion mechanism, the production cross sections

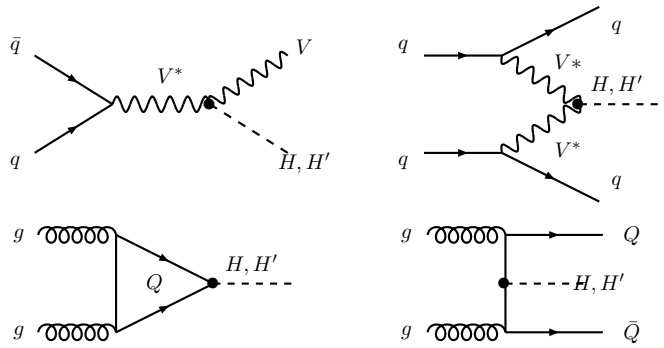

Fig. 3. The dominant Higgs boson production mechanisms in hadronic collisions.

for the light Higgs, H, and the heavy Higgs, H', can be approximated as

$$\sigma_H \propto \alpha_s^2 \left(\frac{m_Q^2}{v^2}\cos^2\theta\right) \times |\eta(\epsilon)|^2 \times (\text{gg luminosity}), \tag{52}$$

$$\sigma_{H'} \propto \alpha_s^2 \left(\frac{m_Q^2}{v^2}\sin^2\theta\right) \times |\eta(\epsilon')|^2 \times (\text{gg luminosity}), \tag{53}$$

where the first bracket is due to the coupling $QQH(H')$. Here, $\epsilon = (4m_Q^2)/(m_H^2)$, $\epsilon' = (4m_Q^2)/(m_{H'}^2)$, and

$$\eta(\epsilon) = \frac{\epsilon}{2}[1 + (\epsilon - 1)\phi(\epsilon)], \tag{54}$$

with

$$\phi(\epsilon) = \begin{cases} -\arcsin^2(1/\sqrt{2}) & \epsilon \leq 1 \\ \frac{1}{4}\left[\log\frac{1+\sqrt{1-\epsilon}}{1-\sqrt{1-\epsilon}} + i\pi\right]^2 & \epsilon > 1 \end{cases} \tag{55}$$

The cross section of the light Higgs production is then reduced relative to the SM one by the factor of $\cos^2\theta$. We also expect that the the heavy Higgs production is typically less than that of the light Higgs by two orders of magnitudes, *i.e.*,

$$\frac{\sigma_{H'}}{\sigma_H} \simeq \frac{\sin\theta^2}{\cos\theta^2}\ \frac{m_H^2}{m_{H'}^2} \simeq \mathcal{O}(10^{-2}). \tag{56}$$

This can be explained by the fact that the heavy Higgs production is suppressed by two factors: the small $\sin\theta$, and the large $m_{H'}$.

The mechanism of Higgs production in association with heavy quark pairs is expressed by additional diagrams shown in Figure 4. The leading order of this process shows that its cross section is less by one order of magnitude than the gluon-gluon fusion process, for $m_{H(H')} < 1$ TeV. Furthermore, the ratio of $\sigma(gg \to H'Q\bar{Q})$ to $\sigma(gg \to HQ\bar{Q})$ is of order $(\sin\theta/\cos\theta)^2 \simeq \mathcal{O}(0.1)$ for $m_H < 300$ GeV.

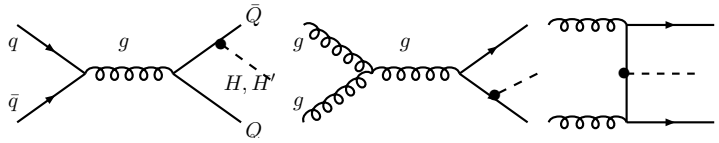

Fig. 4. Feynman diagrams for Higgs production in association with heavy quarks in hadronic collisions, $pp \to q\bar{q}, gg \to Q\bar{Q}H$, at LO.

Finally, we consider the Higgs production in association with $W/Z/Z'$ bosons and in the weak vector boson fusion processes, Equations 50 and 51 respectively. The cross sections of $q\bar{q} \to V + H$ are proportional to the mass of the gauge boson and the mixing angle θ:

$$V \equiv W/Z : \sigma_H \propto \frac{m_V^4}{v^2} \cos^2\theta \times \frac{g^2}{m_V^2} \times F(m_V^2, m_H^2, s), \tag{57}$$

$$\sigma_{H'} \propto \frac{m_V^4}{v^2} \sin^2\theta \times \frac{g^2}{m_V^2} \times F(m_V^2, m_{H'}^2, s). \tag{58}$$

where $F(m_V^2, m_H^2, s)$ is the usual two-body phase space function.

In case of $V \equiv Z'$, The production receives an enhancement factor from the $HZ'Z'$ coupling arising with $m_{Z'}$, and a suppression factor coming from a large value of v' and the mass of the virtual gauge boson(s), $m_{Z'}$:

$$V \equiv Z' : \sigma_H \propto \frac{m_{Z'}^4}{v'^2} \sin^2\theta \times \frac{(g'' Y_{B-L}^Q)^2}{m_{Z'}^2} \times F(m_{Z'}^2, m_H^2, s), \tag{59}$$

$$\sigma_{H'} \propto \frac{m_{Z'}^4}{v'^2} \cos^2\theta \times \frac{(g'' Y_{B-L}^Q)^2}{m_{Z'}^2} \times F(m_{Z'}^2, m_{H'}^2, s). \tag{60}$$

Therefore, $\sigma_H(W/Z)$ can be larger than $\sigma_H(Z')$ by one order of magnitude at most. In contrary, one observes that $\sigma_{H'}(Z') > \sigma_{H'}(W/Z)$. The weak vector boson fusion process, on the other hand, is relatively suppressed due to the extra Vff coupling.

The cross sections for the Higgs bosons production in these channels (Equations 48-51) have been calculated using the FORTRAN codes: HIGLU, HQQ, V2HV, and VV2HV, respectively [15]. Extra subroutines have been added to these programs to account for the new couplings associated with the new particles predicted in this model [15]. The input parameters used in this analysis are given in Table 2. The cross sections for the light Higgs boson production are summarized in Figure 5 as functions of the light Higgs mass with $m_{H'} = 1$ TeV. Figure 6, on the other hand, represents the heavy Higgs productions as functions of $m_{H'}$ with $m_H = 200$ GeV.

As shown in Figure 5, all cross sections of the light Higgs production are reduced by about $25 - 35\%$ in the interesting mass range: $m_H < 250$ GeV. Similar to the SM senario, the main contribution to the production cross section comes from the gluon-gluon fusion mechanism with a few tens of pb. The Higgs production in the

Table 2. Input parameters for the numerical calculation of the Higgs production.

parameter	v	v'	$\sqrt{s}$	$m_{Z'}$
Value (TeV)	0.246	1	14	0.6

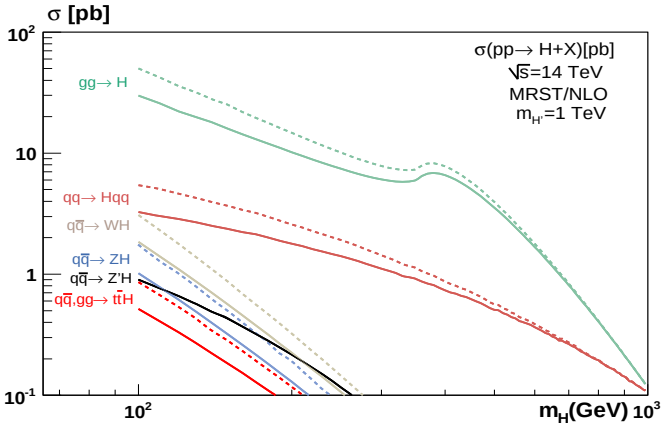

Fig. 5. The cross sections of the light Higgs production as function of m_H: 100 GeV $\leq$ m$_{\rm H}$ $\leq$ 1 TeV, for $m_{H'} = 1$ TeV, $m_{Z'} = 600$ GeV. The solid lines indicate the reduced slope for the minimal $B - L$ extension of the SM.

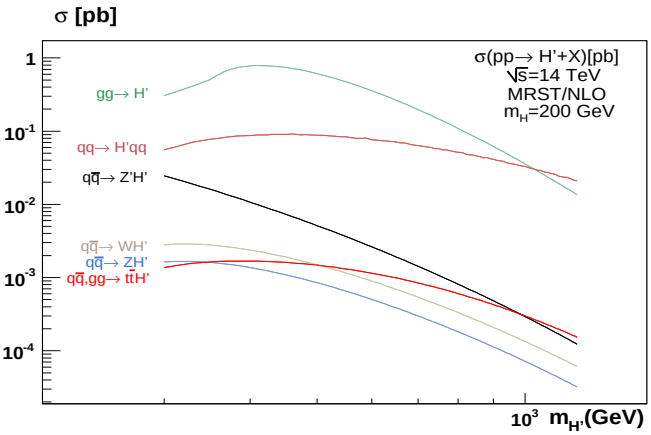

Fig. 6. The cross sections of the heavy Higgs production as function of $m_{H'}$: 300 GeV $\leq$ m$_{\rm H'}$ $\leq$ 1 TeV, for $m_H = 200$ GeV, $m_{Z'} = 600$ GeV.

weak vector boson mechanism, comes next at the level of a few pb. We also notice that the production associated with Z/W dominates the production associated with Z' for $m_H < 300$ GeV.

The production of the heavy Higgs gives very small cross sections relative to the the light Higgs ones. As shown in Figure 6, all these cross sections are scaled down by factor $\mathcal{O}(10^{-2})$.

4.2. *Higgs Decay*

The Higgs decay modes can be categorized into three groups: Higgs decays into fermions (Figure 7), Higgs decays into massive gauge bosons (Figure 8), and Higgs decays into massless gauge bosons (Figure 9).

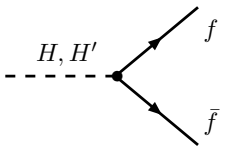

Fig. 7. The Feynman diagram for the Higgs boson decays into fermions.

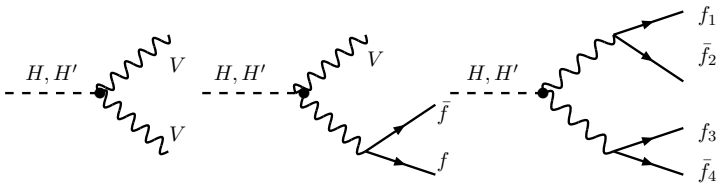

Fig. 8. Diagrams for the Higgs boson decays into massive gauge bosons.

The decay widths into fermions are given by

$$\Gamma(H \longrightarrow ff) \approx m_H \left(\frac{m_f}{v}\right)^2 \left(1 - \frac{4m_f^2}{m_H^2}\right)^{3/2} \cos^2\theta, \tag{61}$$

$$\Gamma(H' \longrightarrow ff) \approx m_{H'} \left(\frac{m_f}{v}\right)^2 \left(1 - \frac{4m_f^2}{m_{H'}^2}\right)^{3/2} \sin^2\theta. \tag{62}$$

In case of the top quark, three-body decays into on-shell and off-shell states (Figure 10) are taken into consideration.

The partial width for H and H' bosons decaying into two real gauge bosons are

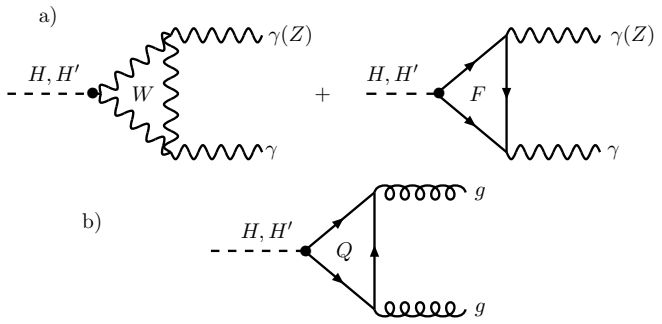

Fig. 9. Loop induced Higgs boson decays into a) two photons ($Z\gamma$) and b) two gluons.

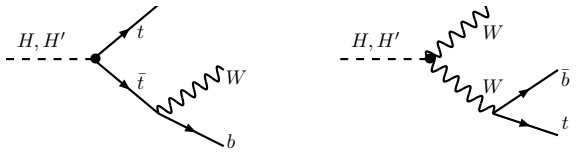

Fig. 10. Diagrams for the three–body decays of the Higgs boson into tbW final states.

given by

$$V \equiv W/Z: \ \Gamma_H \approx \frac{m_H^3}{v^2} f(m_V^2/m_H^2) \cos^2\theta, \quad \Gamma_{H'} \approx \frac{m_{H'}^3}{v^2} f(m_V^2/m_{H'}^2) \sin^2\theta, \quad (63)$$

$$V \equiv Z': \ \Gamma_H \approx \frac{m_H^3}{v'^2} f(m_V^2/m_H^2) \sin^2\theta, \quad \Gamma_{H'} \approx \frac{m_{H'}^3}{v'^2} f(m_V^2/m_{H'}^2) \cos^2\theta, \quad (64)$$

with

$$f(x) = \sqrt{1-4x}(1-4x+12x^2). \quad (65)$$

Three-body and four-body decays are also taken into consideration in the analysis.

The massless gauge bosons couple to the Higgs bosons via W, charged fermions, and quark loops,Figure 9. In this case, the decay widths are relatively suppressed since they are proportional to the HVV and Hff couplings.

From the above Equations, one sees that the new decay mode of $Z'Z'$ has a very small contribution to the total decay width. Thus, one expects that the light Higgs branching ratios in this model of $B-L$ extension should be indistinguishable from the SM case.

The decay widths and branching ratios of the Higgs bosons in these channels have been calculated using the FORTRAN code: HDECAY with extra subroutines for the new couplings associated with the two higgs scalars and the extra gauge boson [16,15]. The input parameters used in this analysis is shown that of the Higgs production analysis (Table 2).

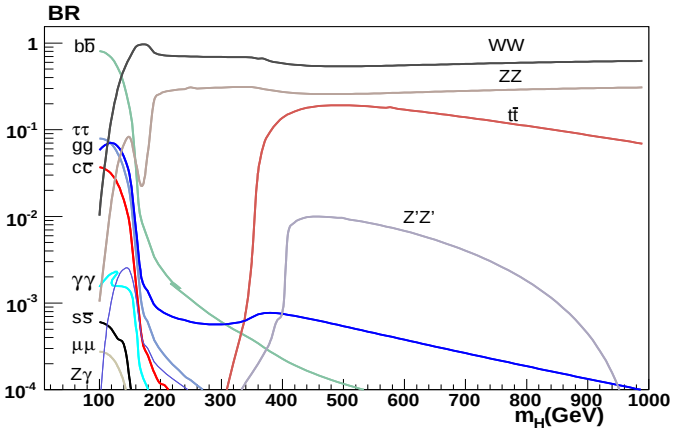

Fig. 11. The branching ratios of the light Higgs decay as function of m_H for $m_{H'} = 1$ TeV, $m_{Z'} = 600$ GeV.

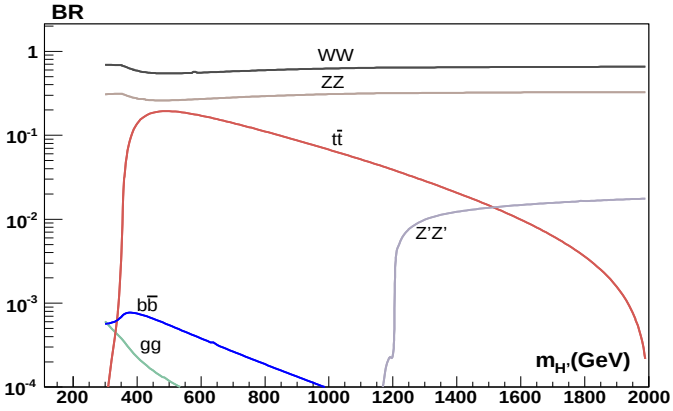

Fig. 12. The branching ratios of the heavy Higgs decay as function of $m_{H'}$ for $m_H = 200$ GeV, $m_{Z'} = 600$ GeV.

The decay branching ratios of the light and heavy Higgs bosons are shown in Figures 11 and 12, respectively, as functions of the Higgs masses. As expected, the branching ratios of the light Higgs are indistinguishable from the SM ones. In the "low mass"range: 100 GeV $< M_H <$ 130 GeV, the main contribution comes from the decay mode $H \to b\bar{b}$ with a branching ratio of $\sim 75 - 50\%$. In the "High mass "range: $m_H >$ 130 GeV, however, the WW, ZZ, and to some extent the $t\bar{t}$ decays give the dominant contributions. The $Z'Z'$ decay arises for small Higgs mass (350 GeV) with a small branching ratio $\lesssim 1\%$ due to the three-body and four-body decays.

Regarding the heavy Higgs decay branching ratio, the decay mode $Z'Z'$ does

not contribute significantly. account for the remaining branching ratios. One also finds that the heavy Higgs may decay to a pair of the lighter Higgs. However, the partial decay width of this channel, which can be expressed by

$$\Gamma(H' \longrightarrow HH) \approx \frac{1}{16\pi\sqrt{2}} \frac{g^2_{H^2H'}}{m_{H'}} \left(1 - \frac{4m^2_{H'}}{m^2_H}\right)^{1/2}, \tag{66}$$

is suppressed by the tiny $g_{H^2H'}$ coupling (Equation 13) and the relatively large $m_{H'}$. In fact, the resulting branching ratio of this decay mode is at the level of 10^{-8}, and hence does not appear in Figure 12.

5. Z' decay in $B - L$ extension of the SM

We now consider the decay of the extra gauge boson predicted by the $B-L$ extension of the SM at LHC. In fact, extra gauge bosons are predicted in many models [17,6]. In some of these models, the mixing between the Z' and the SM Z induces couplings between the extra Z' boson and the SM fermions. In the model we consider in this analysis, there is no tree-level $Z - Z'$mixing. However, the extra $B - L$ Z' boson and the SM fermions are coupled through the $B - L$ quantum numbers.

The interactions of the Z' boson with the SM fermions are described by

$$\mathcal{L}^{Z'}_{\rm int} = \sum_f Y^f_{B-L}\ g''\ Z'_\mu\ f\gamma^\mu f. \tag{67}$$

The decay widths of $Z' \to f\bar{f}$ are then given by [6]

$$\begin{aligned}
\Gamma(Z' \to l^+l^-) &\approx \frac{(g''Y^l_{B-L})^2}{24\pi} m_{Z'} \\
\Gamma(Z' \to q\bar{q}) &\approx \frac{(g''Y^q_{B-L})^2}{8\pi} m_{Z'} \left(1 + \frac{\alpha_s}{\pi}\right),\ q \equiv b, c, s \\
\Gamma(Z' \to t\bar{t}) &\approx \frac{(g''Y^q_{B-L})^2}{8\pi} m_{Z'} \left(1 - \frac{m^2_t}{m^2_{Z'}}\right) \left(1 - \frac{4m^2_t}{m^2_{Z'}}\right)^{1/2} \\
&\quad \left(1 + \frac{\alpha_s}{\pi} + O\left(\frac{\alpha_s m^2_t}{m^2_{Z'}}\right)\right)
\end{aligned} \tag{68}$$

Figure 13 shows the decay branching ratios of Z' as a function of $m_{Z'}$. The branching ratios of $Z' \to l^+l^-$ are relatively high compared to $Z' \to q\bar{q}$. This is, however, not the case in the SM Z decay. This can be explained by $|Y^l_{B-L}| = 3|Y^q_{B-L}|$. Searching for Z' can be then easily achieved at the LHC.

6. Conclusions

In this paper we have presented the phenomenology of the TeV scale $B-L$ extension of the SM at the LHC. We provided a comprehensive analysis for the phenomenology of the SM like Higgs, the extra Higgs scalar, and the extra gauge boson predicted in this model.

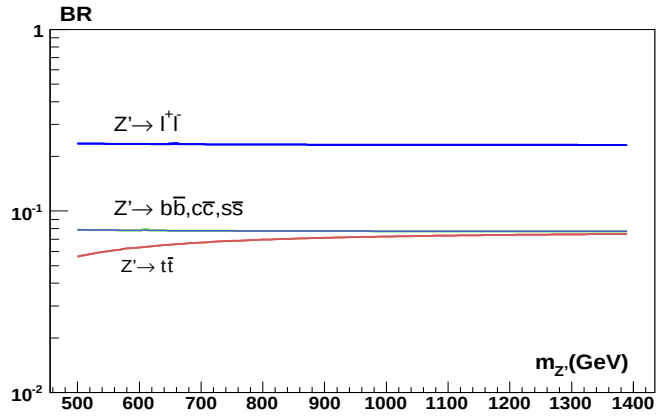

Fig. 13. The decay branching ratios of the extra gauge boson Z' as function of $m_{Z'}$.

We have shown that the cross sections of the SM-like Higgs production are reduced by $\sim 20\% - 30\%$ in the mass range of $\sim 120 - 250$ GeV compared to the SM results. On the other hand, the implications of the $B - L$ extension to the SM do not change the decay branching ratios. Moreover, we found that the extra Higgs has relatively small cross sections, but it is accessible at LHC. Finally, we showed that the branching ratios of $Z' \to l^+l^-$ are of order $\sim 20\%$ compared to $\sim 3\%$ of the SM $BR(Z \to l^+l^-)$.

References

1. R. N. Mohapatra and R. E. Marshak, Phys. Rev. Lett. **44**, 1316 (1980); R. E. Marshak and R. N. Mohapatra, Phys. Lett. B **91**, 222 (1980); C. Wetterich, Nucl. Phys. B **187**, 343 (1981); A. Masiero, J. F. Nieves and T. Yanagida, Phys. Lett. B **116**, 11 (1982); R. N. Mohapatra and G. Senjanovic, Phys. Rev. D **27**, 254 (1983); R. E. Marshak and R. N. Mohapatra, S. S. Rao, W. Buchmuller, C. Greub and P. Minkowski, Phys. Lett. B **267**, 395 (1991).
2. S. Khalil, arXiv:hep-ph/0611205.
3. D. G. Cerdeno, A. Dedes and T. E. J. Underwood, JHEP **0609** (2006) 067 [arXiv:hep-ph/0607157];
   W. F. Chang, J. N. Ng and J. M. S. Wu, arXiv:hep-ph/0701254.
4. D. O'Connell, M. J. Ramsey-Musolf and M. B. Wise, Phys. Rev. D **75**, 037701 (2007) [arXiv:hep-ph/0611014].
5. A. Datta and A. Raychaudhuri, Phys. Rev. D **57**, 2940 (1998) [arXiv:hep-ph/9708444].
6. M. Carena, A. Daleo, B. A. Dobrescu and T. M. P. Tait, Phys. Rev. D **70**, 093009 (2004).
7. M.Abbas and S.Khalil, arXiv:hep-ph/0707.0841, submitted to Eur.Phys.J.C.
8. M. Altmann *et al.* [GNO COLLABORATION Collaboration], Phys. Lett. B **616**, 174 (2005); B. Aharmim *et al.* [SNO Collaboration], Phys. Rev. D **72**, 052010 (2005); T. Araki *et al.* [KamLAND Collaboration], Phys. Rev. Lett. **94**, 081801 (2005); Y. Ashie *et al.* [Super-Kamiokande Collaboration], Phys. Rev. D **71**, 112005 (2005); E. Aliu *et*

al. [K2K Collaboration], Phys. Rev. Lett. **94**, 081802 (2005); P. Adamson *et al.* [MINOS Collaboration], Phys. Rev. D **73**, 072002 (2006); M. Ambrosio *et al.* [MACRO Collaboration], Eur. Phys. J. C **36**, 323 (2004).

9. R. N. Mohapatra *et al.*, arXiv:hep-ph/0510213; R. N. Mohapatra and A. Y. Smirnov, Ann. Rev. Nucl. Part. Sci. **56** (2006) 569;A. Strumia and F. Vissani, arXiv:hep-ph/0606054.
10. A. Djouadi, arXiv:hep-ph/0503172.
11. H. M. Georgi, S. L. Glashow, M. E. Machacek and D. V. Nanopoulos, Phys. Rev. Lett. **40**, 692 (1978).
12. R. Raitio and W. W. Wada, Phys. Rev. D **19**, 941 (1979); J. N. Ng and P. Zakarauskas, Phys. Rev. D **29**, 876 (1984); D. A. Dicus and S. Willenbrock, Phys. Rev. D **39**, 751 (1989).
13. S. L. Glashow, D. V. Nanopoulos and A. Yildiz, Phys. Rev. D **18** (1978) 1724; J. Finjord, G. Girardi and P. Sorba, Phys. Lett. B **89**, 99 (1979); E. Eichten, I. Hinchliffe, K. D. Lane and C. Quigg, Rev. Mod. Phys. **56**, 579 (1984) [Addendum-ibid. **58**, 1065 (1986)].
14. D. A. Dicus and S. S. D. Willenbrock, Phys. Rev. D **32**, 1642 (1985); R. N. Cahn and S. Dawson, Phys. Lett. B **136**, 196 (1984) [Erratum-ibid. B **138**, 464 (1984)]; W. Kilian, M. Kramer and P. M. Zerwas, Phys. Lett. B **373**, 135 (1996) [arXiv:hep-ph/9512355].
15. The FORTRAN codes: HIGLU, HQQ, V2HV, and VV2HV have been written by M. Spira and can be found at http://people.web.psi.ch/spira/proglist.html. The modefied version was made by W. Emam and can be found at http://www.bue.edu.eg/centres/ctp/people/codes/proglist.html.
16. A. Djouadi, J. Kalinowski and M. Spira, Comput. Phys. Commun. **108**, 56 (1998) [arXiv:hep-ph/9704448].
17. J. L. Hewett and T. G. Rizzo, Phys. Rep. **183**, 139 (1989); M. Cvetic and S. Godfrey, arXiv:hep-ph/9504216; A. Leike, Phys. Rept. **317**, 143 (1999).
18. E. Boos, A. Djouadi, M. Muhlleitner and A. Vologdin, Phys. Rev. D **66**, 055004 (2002) [arXiv:hep-ph/0205160].
19. M. Krawczyk, P. Mattig and J. Zochowski, Eur. Phys. J. C **19**, 463 (2001). [arXiv:hep-ph/0009201].
20. C. Boehm, J. Orloff and P. Salati, Phys. Lett. B **641**, 247 (2006) [arXiv:astro-ph/0607437].